JOURNAL OF NATURAL PRODUCTS

Article

pubs.acs.org/jnp

Structural Characterization and Assessment of the Cytotoxicity of 2,3-Dihydro-1*H*-indene Derivatives and Coumarin Glucosides from the Bark of *Streblus indicus*

Ruijie He,[†,‡] Xishan Huang,[§] Yanjun Zhang,[†] Liangdeng Wu,[†] Hui Nie,[†] Dexiong Zhou,[†] Buming Liu,[⊥] Shengping Deng,[†] Ruiyun Yang,[†] Shuai Huang,[†] Zhijie Nong,[†] Jun Li,*[,†] and Yan Huang*[,⊥]

[†]State Key Laboratory for the Chemistry and Molecular Engineering of Medicinal Resources, College of Chemistry and Pharmacy, Guangxi Normal University, Guilin 541004, People's Republic of China

[‡]Guangxi Key Laboratory of Functional Phytochemicals Research and Utilization, Guangxi Institute of Botany, Guilin 541006, People's Republic of China

[§]School of Chemistry and Chemical Engineering, Sun Yat-sen University, Guangzhou 510275, People's Republic of China

[⊥]Guangxi Key Laboratory of Traditional Chinese Medicine Quality Standards, Nanning 530022, People's Republic of China

Supporting Information

ABSTRACT: A pair of enantiomers and a pair of 2,3-dihydro-1*H*-indene epimers, *rac*-indidene A (*rac*-**1**), indidenes B and C (**2**, **3**); four new coumarin glucosides (**4**−**7**); and four known coumarin glucosides (**8**−**11**) were isolated from the bark of *Streblus indicus* (Bur.) Corner. The structures of **1**−**11** were defined by physical data analyses, including MS, NMR, and single-crystal X-ray diffraction. The absolute configurations of the 2,3-dihydro-1*H*-indene derivatives were defined via experimental and calculated ECD data. *rac*-Indidene A and indidenes B and C showed inhibitory activity against A549 and MCF-7 tumor cells with IC_{50} values in the range of 2.2 ± 0.1 to 7.2 ± 0.9 μM.

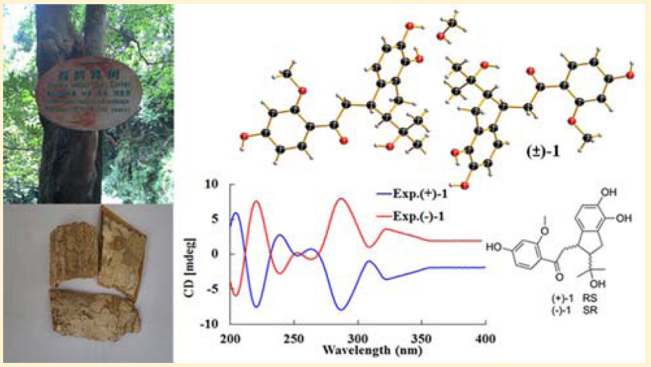

Streblus indicus (Bur.) Corner, a perennial arbor of the Moraceae family, is widespread in South Asia, particularly in southern China.[1] The bark of *S. indicus*, "Zhi Xie Shu Pi" in Chinese, is often used for hemostasis and the treatments of inflammation and various rheumatoid diseases.[2,3] The *S. indicus* plant contains large amounts of coumarins, which have been demonstrated as bioactive substances corresponding to the traditional application of this plant.[2,3] The coumarin derivatives have also been reported to have potent cytotoxic activities,[4−6] prompting further investigation of more structurally attractive or bioactive coumarin derivatives from this plant. As part of an ongoing project to identify the bioactive metabolites from this genus,[7−18] the extracts of *S. indicus* were examined, and the results of bioactive screening indicated that the EtOAc extract exhibited significant cytotoxic inhibitory activity of less than 50 μg/mL. These findings led to the isolation of four 2,3-dihydro-1*H*-indene derivatives and eight coumarin glucosides. To date, no 2,3-dihydro-1*H*-indene derivatives have been obtained from prior phytochemical work on *Streblus asper* plants.[2,19] In the present study, the isolation and structural elucidation of eight new compounds and cytotoxic assessment of these isolates are reported in detail.

RESULTS AND DISCUSSION

The EtOAc fractionation and purification of the 75% EtOH extract of *S. indicus* bark using various chromatographic methods yielded four 2,3-dihydro-1*H*-indene derivatives and eight coumarin glucosides. The structures of **1**−**7** are shown in Chart 1. The four known coumarin glucosides **8**−**11** were identified as 7-*O*-(6-*O*-syringoyl-β-D-glucopyranosyl)-6-methoxycoumarin,[20] skimmin,[21] scopolin,[22] and 7-*O*-(6-*O*-sinapoyl-β-D-glucopyranosyl)-6-methoxycoumarin,[20] respectively.

Indidene A (**1**) was obtained as colorless crystals (MeOH) with $[\alpha]_D^{25}$ 0.01 (*c* 0.4, MeOH). A sodium adduct ion at *m*/*z* 395.14560 $[M + Na]^+$ (calcd for $C_{21}H_{24}O_6Na$, 395.14706) observed in the positive-ion HRESIMS indicated a molecular formula of $C_{21}H_{24}O_6$. The ^1H NMR data (Table 1) revealed a 1,2,4-trisubstituted aromatic moiety at δ_H 6.47 (d, *J* = 2.1 Hz, H-3‴), 6.42 (dd, *J* = 8.5, 2.1 Hz, H-5‴), and 7.67 (d, *J* = 8.5 Hz, H-6‴); two *ortho*-coupled aromatic protons at δ_H 6.55 (d, *J* = 8.5 Hz, H-6′) and 6.44 (d, *J* = 8.5 Hz, H-7′); one methoxy group at δ_H 3.84 (s, 2‴-OMe); two methyl groups at δ_H 1.06 (s, Me-1″) and 1.04 (s, Me-3″); two methylene groups at δ_H 2.98 (dd, *J* = 17.0, 8.9 Hz, H-3′a), 2.82 (dd, *J* = 17.0, 3.7 Hz, H-3′b),

Received: April 7, 2016

DOI: 10.1021/acs.jnatprod.6b00306
J. Nat. Prod. XXXX, XXX, XXX−XXX

Chart 1. Structures of 1−7

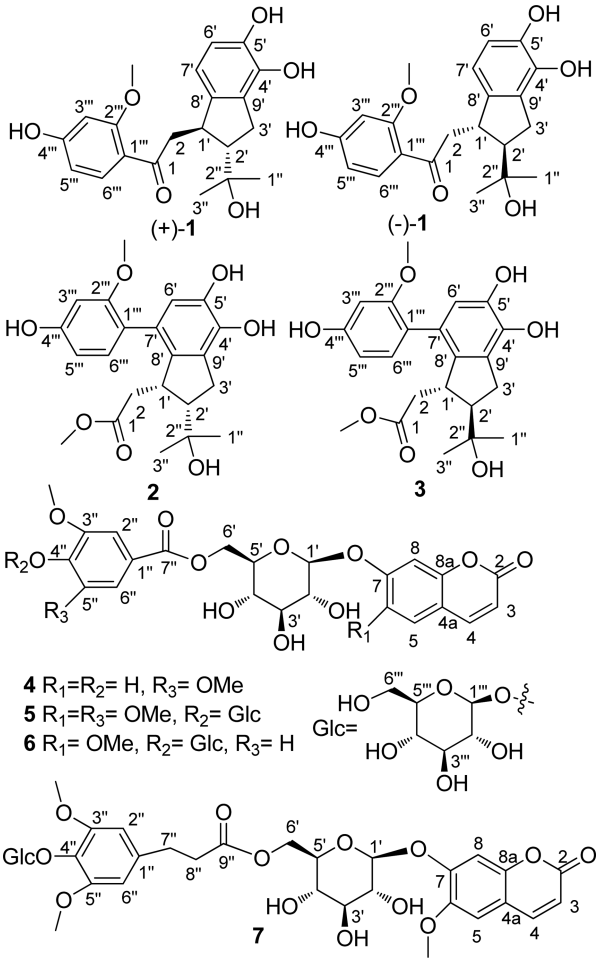

and δ_H 3.26 (m, H-2); and two methine groups at δ_H 3.64 (td, J = 6.8, 3.4 Hz, H-1′) and 2.26 (td, J = 8.9, 3.7 Hz, H-2′). The ^{13}C NMR data (Table 1) displayed 21 carbon resonances that were identified by HSQC as nine nonprotonated carbons (one ketocarbonyl carbon, seven olefinic carbons, and one sp^3 oxygen-bearing carbon); seven methine carbons (five olefinic carbons and two sp^3 carbons); two sp^3 methylene carbons; and three methyl carbons. The ^{1}H−^{1}H COSY cross-peaks (Figure 1) of H_2-2/H-1′/H-2′/H_2-3′ and the HMBC correlations of H-7′/C-1′; H_3-3′/C-4′, C-8′, C-9′, C-2″; and H-2′/C-8′, C-2″, C-9′ indicated that C-1′, C-2′, and C-3′ were linked to C-8′, C-2″, and C-9′, respectively. The H-1′/H-6‴ correlations with the carbonyl carbon (δ_C 202.5) in the HMBC spectrum indicated that C-2 and C-1‴ were linked via a carbonyl carbon (Figure 1). The connectivity of the methoxy group with C-2‴ was demonstrated by the methoxy protons (δ_H 3.84) /C-2‴ (δ_C 163.0) and H-5‴ (δ_H 6.42)/C-4‴ (δ_C 165.0) HMBC correlations. The HMBC correlations of H-1″/C-2′, C-2″, C-3″ and H-3″/C-2′, C-1″, C-2″ revealed the linkages of C-1″ and C-3″ with C-2″. The hydroxy groups at C-4′, C-5′, C-2″, and C-4‴ were verified via the HRESIMS data and supported by the chemical shifts of C-4′ (δ_C 141.9), C-5′ (δ_C 144.7), C-2″ (δ_C 74.0), and C-4‴ (δ_C 165.0). Based on these results, the structure of compound **1**, indidene A, was defined as 2-[4,5-dihydroxy-2-(2-hydroxypropan-2-yl)-2,3-dihydro-1*H*-inden-1-yl]-1-(4-hydroxy-2-methoxyphenyl)ethanone.

The structure of indidene A was confirmed using X-ray crystallographic diffraction (Figure 2). The centrosymmetric space group $P\bar{1}$ (n = 2) indicated a racemic mixture, congruent with the near zero optical rotation. The chiral HPLC separation of *rac*-**1** using a Chiralpak AD-H column revealed the presence of two enantiomers, (+)-**1** and (−)-**1**, with opposite Cotton effects (Figure 3) and opposite optical rotations. To determine the absolute configurations of (+)-**1** and (−)-**1**, the ECD spectra of (+)-**1** and (−)-**1** were measured in MeOH and compared with the calculated ECD spectra of the enantiomers. The experimental ECD spectrum of (+)-**1** was consistent with the calculated ECD spectrum of (1′*R*, 2′*S*)-**1**. Thus, the absolute configurations of (+)-**1** and (−)-**1** were elucidated as 1′*R*,2′*S* and 1′*S*,2′*R*, respectively. The complete structures of (+)-indidene A (**1**) and (−)-indidene A (**1**) were established as depicted in Chart 1.

Indidene B (**2**) was isolated as pale red powder. The positive-ion HRESIMS data (m/z, 425.15618 [M + Na]$^+$, calcd for $C_{22}H_{26}O_7Na$, 425.15762) suggested a molecular formula of $C_{22}H_{26}O_7$, that is, one more CH_2O unit than **1**. Comparison between the NMR data of **2** and **1** (Table 1) revealed that the 4-hydroxy-2-methoxyphenyl group at C-1 in **1** was replaced by a methoxy group in **2**, and the 4-hydroxy-2-methoxyphenyl group shifted to C-7′ in **2**. This was confirmed by the HRESIMS data and the correlations of the methoxy protons (δ_H 3.51) with the ester carbonyl carbon (δ_C 175.0), H-6‴ (δ_H 6.90) with C-7′ (δ_C 127.9), and H-6′ (δ_H 6.45) with C-1‴ (δ_C 122.4) in the HMBC spectrum (Figure 1), as well as the chemical shifts of the C═O group and C-7′ that shifted from δ_C 202.5 and 115.8 in **1** to δ_C 175.0 and 127.9 in **2**, respectively. Therefore, the 2D structure of **2** was established. Based on the ROESY correlations (Figure 1) of H_2-2 with H_3-1″/3″, the C-1′/C-2′ relative configuration was determined as *cis*. The absolute configuration of **2** was determined via the experimental and calculated ECD data. The atropisomerism of **2** was investigated by a 1D potential energy surface scan of the C-6′−C-7′−C-1‴−C-6‴ dihedral angle. The minimum conversion energy for *P* and *M* atropisomers was less than 20 kcal/mol (Figure S49, Supporting Information), suggesting that **2** exists as a single compound with interconverting *P* and *M* atropisomers at room temperature.[23] The experimental and calculated ECD data permitted assignment of the absolute configuration of the C-1′ and C-2′ stereogenic centers of **2** as 1′*S*,2′*S* (Figure 4). Thus, the structure of indidene B (**2**) was established as methyl 2-[(1*S*,2*S*)-4,5-dihydroxy-7-(4-hydroxy-2-methoxyphenyl)-2-(2-hydroxypropan-2-yl)-2,3-dihydro-1*H*-inden-1-yl]acetate.

Based on the HRESIMS data analysis, the molecular formula of indidene C (**3**) was established as $C_{22}H_{26}O_7$, the same as that of indidene B (**2**). It exhibited NMR data similar to that of indidene B (**2**) (Table 1), suggesting that **3** shared the same 2D structure with **2**. The ROESY correlations of H-1′ with H_3-1″/3″ defined the 1′,2′-*trans* relative configuration of **3**. Similar to **2**, the minimum energy for the conversion of *P* and *M* atropisomers of **3** was also below 20 kcal/mol (Figure S50, Supporting Information), indicating the fast interconversion of its *P* and *M* conformers. The experimental and calculated ECD data (Figure 5) suggested that the absolute configuration of **3** was 1′*S*,2′*R*. Therefore, the structure of indidene C (**3**) was established as methyl 2-[(1*S*,2*R*)-4,5-dihydroxy-7-(4-hydroxy-2-methoxyphenyl)-2-(2-hydroxypropan-2-yl)-2,3-dihydro-1*H*-inden-1-yl]acetate.

DOI: 10.1021/acs.jnatprod.6b00306
J. Nat. Prod. XXXX, XXX, XXX−XXX

Table 1. NMR Data (500 MHz, Methanol-d_4, δ in ppm) of Indidenes A–C (1–3)

	indidene A (1)		indidene B (2)		indidene C (3)	
position	δ_C, type	δ_H (J in Hz)	δ_C, type	δ_H (J in Hz)	δ_C, type	δ_H (J in Hz)
C=O	202.5, C		175.0, C		175.0, C	
2a	52.8, CH_2	3.26, m	40.63, CH_2	2.16, dd (15.1, 3.4)	40.60, CH_2	2.14, dd (15.0, 3.5)
2b				2.06, dd (15.1, 10.3)		2.02, dd (15.0, 10.2)
1′	44.2, CH	3.64, td (6.8, 3.4)	44.61, CH	3.47, ddd (10.3, 3.4, 1.6)	44.57, CH	3.47, ddd (10.2, 3.5, 1.5)
2′	57.0, CH	2.26, dt (8.9, 3.7)	56.0, CH	2.22, dt (5.3, 1.6)	56.0, CH	2.22, dt (5.3, 1.5)
3′a	31.2, CH_2	2.98, dd (17.0, 8.9)	30.8, CH_2	2.98, d (5.3)	30.8, CH_2	2.96, d (5.3)
3′b		2.82, dd (17.0, 3.7)				
4′	141.9, C		140.9, C		140.9, C	
5′	144.7, C		144.9, C		144.9, C	
6′	115.2, CH	6.55, d (8.5)	117.3, CH	6.45, s	117.3, CH	6.43, s
7′	115.8, CH	6.44, d (8.5)	127.9, C		127.9, C	
8′	140.6, C		137.8, C		137.8, C	
9′	130.7, C		130.6, C		130.6, C	
1″	27.5, CH_3	1.06, s	27.0, CH_3	1.13, s	27.0, CH_3	1.13, s
2″	74.0, C		74.1, C		74.1, C	
3″	26.45, CH_3	1.04, s	26.1, CH_3	1.04, s	26.1, CH_3	1.04, s
1‴	120.9, C		122.4, C		122.4, C	
2‴	163.0, C		158.7, C		158.7, C	
3‴	99.9, CH	6.47, d (2.1)	100.1, CH	6.50, d (1.7)	100.1, CH	6.48, d (1.7)
4‴	165.0, C		159.0, C		159.0, C	
5‴	109.0, CH	6.42, dd (8.5, 2.1)	108.0, CH	6.42, dd (8.1, 1.7)	108.0, CH	6.41, dd (8.1, 1.7)
6‴	133.9, CH	7.67, d (8.5)	132.6, CH	6.90, d (8.1)	132.6, CH	6.89, d (8.1)
CH_3O-2‴	56.0, CH_3	3.84, s	55.6, CH_3	3.73, s	55.6, CH_3	3.72, s
CH_3O-			51.9, CH_3	3.51, s	51.9, CH_3	3.51, s

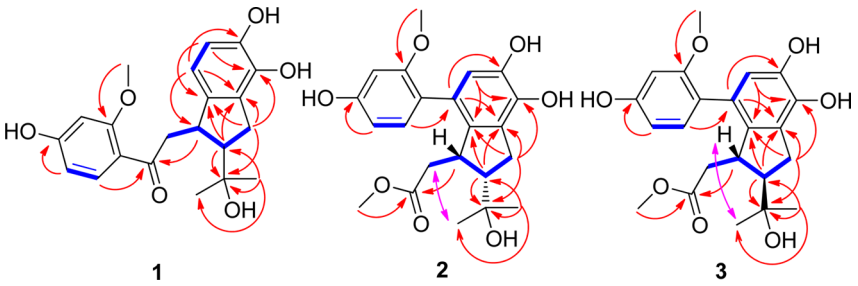

Figure 1. HMBC (arrows), $^1H-^1H$ COSY (bonds), and ROESY (double arrows) correlations of **1**–**3**.

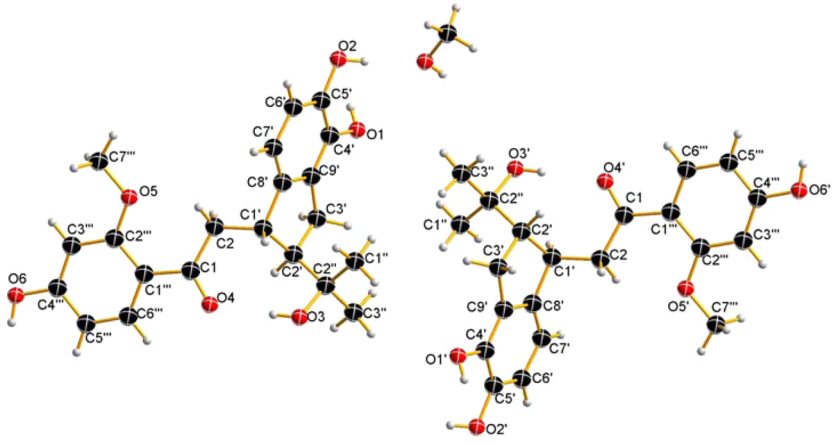

Figure 2. ORTEP drawing of **1**.

The molecular formula of indidene D (**4**) was $C_{24}H_{24}O_{12}$ based on the sodium adduct ion at m/z 527.11545 $[M + Na]^+$ (calcd for $C_{24}H_{24}O_{12}Na$ 527.11655) in its HRESIMS. Comparison of its NMR data (Tables 2 and 3) with those of 7-*O*-(6-*O*-syringoyl-β-D-glucopyranosyl)-6-methoxycoumarin (**8**)[20] revealed that the C-6 methoxy signal (δ_H 3.79, δ_C 56.1) in

DOI: 10.1021/acs.jnatprod.6b00306
J. Nat. Prod. XXXX, XXX, XXX–XXX

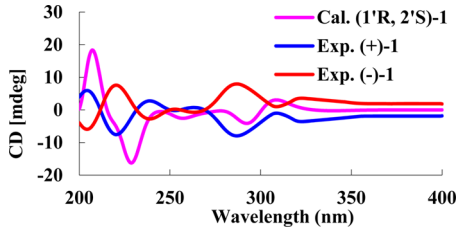

Figure 3. Experimental ECD spectra of (+)-**1** and (−)-**1** and calculated ECD spectrum of (1′*R*,2′*S*)-**1**.

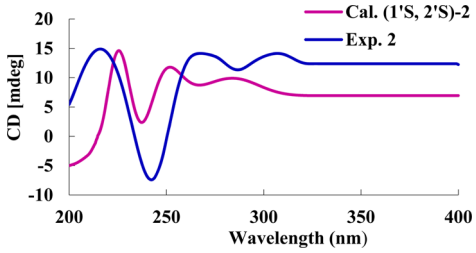

Figure 4. Experimental ECD spectrum of 2 and calculated ECD spectrum of (1′*S*,2′*S*)-2.

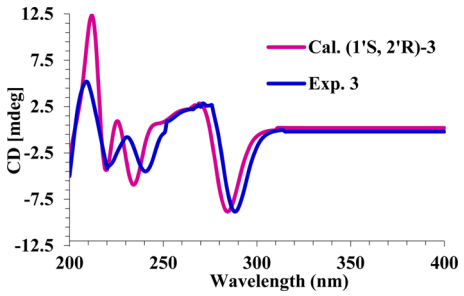

Figure 5. Experimental ECD spectrum of **3** and calculated ECD spectrum of (1′*S*,2′*R*)-**3**.

8 was replaced by an aromatic proton signal (δ_H 7.00) in **4**. The molecular formula, the 32.8 ppm upfield shift of C-6 (δ_C 113.2), the 10.1 ppm downfield shift of C-7 (δ_C 159.7), and the correlation of H-6 (δ_H 7.00) with C-7 (δ_C 159.7) in the HMBC spectrum (Figure 6) supported these changes in **4**. The hydrolysis of **4** in 1 M HCl yielded D-glucose, as determined by TLC and GC analyses (see Experimental Section). The coupling constant between H-1′ and H-2′ of 7.5 Hz indicated the *β*-anomeric configuration for **4**. The structure of **4** was therefore established as 7-*O*-(6-*O*-syringoyl-*β*-D-glucopyranosyl)coumarin and named indidene D.

Indidene E (**5**) gave a sodium adduct ion at *m*/*z* 719.17989 $[M + Na]^+$ (calcd for $C_{31}H_{36}O_{18}Na$, 719.17993) in the positive-ion HRESIMS, which suggested a molecular formula of $C_{31}H_{36}O_{18}$. The NMR data (Tables 2 and 3) of **5** were highly similar to those of 7-*O*-(6-*O*-syringoyl-*β*-D-glucopyranosyl)-6-methoxycoumarin (**8**),[20] except for the additional signals for one glucosyl moiety at δ_H 5.11 and δ_C 102.6, 74.2, 77.3, 69.8, 76.6, and 60.7. The shielded C-4″ resonance (δ_C 138.7), deshielded C-3″/C-5″ resonances (δ_C 152.2), and the correlation of Glc-H-1‴ (δ_H 5.11) with C-4″ (δ_C 138.7) in the HMBC spectrum (Figure 6) supported this conclusion. The acid hydrolysis and subsequent TLC and GC analyses revealed that **5** contained two D-glucopyranosyl moieties, the coupling constants of H-1′ (7.4 Hz) and H-1‴ (7.3 Hz) reminiscent of *β*-anomeric configurations. Thus, the structure of **5**, indidene E, was established as 7-[6-(4-*O*-*β*-D-glucopyranosyloxy-3,5-dimethoxybenzoyl)]-*O*-*β*-D-glucopyranosyloxy-6-methoxycoumarin.

Table 2. ^{1}H NMR Data (500 MHz, DMSO-d_6, δ in ppm) for Indidenes D−G (4−7)[a]

	indidene D (**4**)	indidene E (**5**)	indidene F (**6**)	indidene G (**7**)
position	δ_H (*J* in Hz)	δ_H (*J* in Hz)	δ_H (*J* in Hz)	δ_H (*J* in Hz)
3	6.30, d (9.5)	6.31, d (9.5)	6.32, d (9.5)	6.25, d (9.5)
4	7.95, d (9.5)	7.93, d (9.5)	7.99, d (9.5)	7.89, d (9.5)
5	7.50, d (8.6)	7.27, s	7.31, s	7.27, s
6	7.00, dd (8.6, 2.3)			
8	7.04, d (2.3)	7.21, s	7.27, s	7.16, s
1′	5.18, d (7.5)	5.26, d (7.4)	5.24, d (7.4)	5.18, d (7.3)
2′	3.31*	3.34, m	3.36, m	3.32*
3′	3.35, m	3.36, m	3.38, m	3.20, m
4′	3.26, dd (8.8, 4.9)	3.29 dd (8.5, 4.9)	3.25, dd (9.1, 5.2)	3.13, dd (8.6, 4.8)
5′	3.89, ddd (8.8, 7.1, 1.7)	3.92, ddd (8.5, 6.3, 1.7)	3.95, ddd (9.1, 8.0, 1.6)	3.80, ddd (8.6, 7.0, 1.7)
6′a	4.63, d (11.8)	4.60, d (12.0)	4.66, d (11.8)	4.31, d (11.8)
6′b	4.19, dd (11.8, 7.1)	4.24, dd (12.0, 6.3)	4.08, dd (11.8, 8.0)	4.07, dd (11.8, 7.0)
2″	7.16, d (2.0)	7.16, d (2.0)	7.44, d (2.0)	6.39, d (2.0)
5″			7.19, d (8.4)	
6″	7.16, d (2.0)	7.16, d (2.0)	7.57, dd (8.4, 2.0)	6.39, d (2.0)
7″				2.70, m
8″				2.61, m
1‴		5.11, d (7.3)	5.05, d (7.4)	4.80, d (7.4)
2‴		3.22, dd (9.4, 5.3)	3.28, dd (8.6, 5.1)	3.20, m
3‴		3.06, dd (9.4, 5.3)	3.39, dd (8.6, 5.1)	3.02, ddd (9.0, 5.4, 2.0)
4‴		3.14, ddd (9.4, 8.7, 1.9)	3.25, dd (9.1, 5.1)	3.19, m
5‴		3.20, dd (8.7, 4.8)	3.30, dd (9.3, 3.5)	3.35[a]
6‴a		3.55, dd (11.7, 5.6)	3.53, dd (9.3, 5.9)	3.59, dd (9.8, 4.8)
6‴b		3.40, dd (11.7, 5.6)		3.43, m
CH_3O-6		3.79, s	3.82, s	3.81, s
CH_3O-3″	3.74, s	3.74, s	3.77, s	3.66, s
CH_3O-5″	3.74, s	3.74, s		3.66, s

[a]Asterisk indicates overlapped signals.

The molecular formula of $C_{30}H_{34}O_{17}$ of indidene F (**6**) was deduced from its sodium adduct ion in the positive-ion HRESIMS at *m*/*z* 689.16847 $[M + Na]^+$ (calcd for $C_{30}H_{34}O_{17}Na$, 689.16937), which was 30 mass units less than that of **5**. The NMR data of **6** (Tables 2 and 3) were similar to those of **5**, except for the absence of the signals for the C-5″ methoxy group, which was supported by its HRESIMS data, the 11.8 ppm downfield shift of C-4″ (δ_C 150.5), the 38.3 ppm upfield shift of C-5″ (δ_C 113.2), and the correlations of H-5″ with C-1″/C-4″ in the HMBC spectrum (Figure 6). The acid hydrolysis revealed that **6** had the same sugar units as **5**. Compound **6**, indidene F, was therefore characterized as 7-[6-(4-*O*-*β*-D-glucopyranosyloxy-3-methoxybenzoyl)]-*O*-*β*-D-glucopyranosyloxy-6-methoxycoumarin.

The molecular formula of indidene G (**7**) was $C_{33}H_{40}O_{18}$, a C_2H_4 unit more than that of **5**, based on its HRESIMS data. Comparison between the NMR data of **7** and **5** (Tables 2 and

DOI: 10.1021/acs.jnatprod.6b00306
J. Nat. Prod. XXXX, XXX, XXX−XXX

Table 3. ^{13}C NMR Data (125 MHz, DMSO-d_6, δ in ppm) for Indidenes D–G (4–7)

	indidene D (4)	indidene E (5)	indidene F (6)	indidene G (7)
position	δ_C, type	δ_C, type	δ_C, type	δ_C, type
2	160.0, C	160.3, C	160.7, C	160.4, C
3	113.1, CH	113.9, CH	113.3, CH	113.3, CH
4	144.0, CH	144.0, CH	144.3, CH	144.0, CH
4a	113.6, C	112.3, C	112.4, C	112.3, C
5	129.3, CH	110.3, CH	110.1, CH	109.7, CH
6	113.2, CH	145.9, C	145.9, C	145.9, C
7	159.7, C	149.9, C	149.7, C	149.5, C
8	103.0, CH	103.1, CH	102.8, CH	103.0, CH
8a	154.5, C	148.8, C	148.9, C	148.8, C
1′	99.4, CH	101.9, CH	99.2, CH	99.1, CH
2′	73.0, CH	72.9, CH	72.8, CH	72.9, CH
3′	76.1, CH	76.3, CH	76.4, CH	76.5, CH
4′	70.1, CH	69.84, CH	70.0, CH	70.0, CH
5′	73.9, CH	73.7, CH	73.1, CH	73.7, CH
6′	64.0, CH_2	64.2, CH_2	64.5, CH_2	63.7, CH_2
1″	119.2, C	124.4, C	122.6, C	136.0, C
2″	107.0, CH	107.3, CH	112.5, CH	106.2, CH
3″	147.5, C	152.2, C	148.5, C	152.3, C
4″	140.9, C	138.7, C	150.5, C	132.8, C
5″	147.5, C	152.2, C	113.9, CH	152.3, C
6″	107.0, CH	107.3, CH	123.1, CH	106.2, CH
7″	165.4, C	165.7, C	165.3, C	30.4, CH_2
8″				35.0, CH_2
9″				172.1, C
1‴		102.6, CH	99.0, CH	102.9, CH
2‴		74.2, CH	73.7, CH	74.2, CH
3‴		77.3, CH	76.9, CH	77.1, CH
4‴		69.8, CH	69.2, CH	69.9, CH
5‴		76.6, CH	76.7, CH	76.5, CH
6‴		60.7, CH_2	60.3, CH_2	60.7, CH_2
CH_3O-6		56.3, CH_3	56.0, CH_3	56.0, CH_3
CH_3O-3″	56.0, CH_3	56.0, CH_3	55.5, CH_3	56.2, CH_3
CH_3O-5″	56.0, CH_3	56.0, CH_3		56.2, CH_3

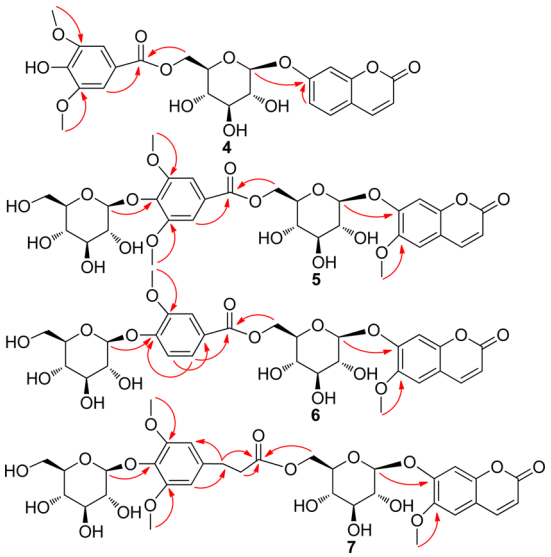

Figure 6. HMBC (arrows) correlations of 4–7.

3) revealed that C-1″ of 7 was linked to the ester carbonyl carbon via a CH_2CH_2 unit. This conclusion was confirmed by the deshielded C-1″ resonance ($\Delta\delta_C$ +11.6) and the deshielded ester carbonyl resonance ($\Delta\delta_C$ +6.4), the H-7″ (δ_H 2.70)/H-8″ (δ_H 2.61) TOCSY correlation, and the H-7″/C-1″, C-6″, C-8″, C-9″; H-8″/C-1″, C-7″, C-9″ correlations in the HMBC spectrum (Figure 6). Thus, the structure of 7, indidene G, was unambiguously established as 7-[6-(4-*O*-β-D-glucopyranosyloxydihydrosinapoyl)]-*O*-β-D-glucopyranosyloxy-6-methoxycoumarin.

All compounds isolated from the bark of *S. indicus* were subjected to MTT assays to assess the cytotoxic activities of these isolates against human lung epithelial A549 and human breast adenocarcinoma MCF-7 cells. As shown in Table 4, *rac*-**1**, **2**, and **3** exhibited cytotoxic activities against A549 and MCF-7 cells with IC_{50} values ranging from 2.2 ± 0.1 to 7.2 ± 0.9 μM.

Table 4. Cytotoxicity Data for the Compounds Isolated from *S. indicus* (IC_{50} ± SD, μM)[a]

compound	A549	MCF-7
(+)-**1**	2.5 ± 0.3	3.9 ± 0.7
(−)-**1**	2.2 ± 0.1	3.3 ± 0.4
2	5.6 ± 0.5	6.7 ± 0.6
3	6.0 ± 0.4	7.2 ± 0.9
paclitaxel	0.02 ± 0.01	0.1 ± 0.03

[a]Other compounds were inactive (IC_{50} > 10 μM).

EXPERIMENTAL SECTION

General Experimental Procedures. Melting points were acquired with an X-6 micromelting point apparatus and are uncorrected. The optical rotations in MeOH were obtained with an ADP440+ polarimeter (λ = 589 nm, path length = 1.0 cm). The UV spectra were measured in MeOH on a TU-1901 spectrophotometer. The ECD spectra were recorded in MeOH on a JASCO J-180 spectropolarimeter. The IR spectra were obtained using a Nicolet Avatar 360 FT-IR spectrometer. The NMR spectra were acquired on a Bruker Advance 500 spectrometer, and the residual solvent peaks of methanol-d_4 (δ_H 3.31 and δ_C 49.00) or DMSO-d_6 (δ_H 2.50 and δ_C 39.52) were used as references. The ESIMS and HRESIMS data were carried out on a Bruker HCT mass spectrometer and MAT 95XP mass spectrometer, respectively. GC was run on an Agilent 7890AGC system. Analytical HPLC was conducted on an Agilent 1200 HPLC system using a 4.6 i.d. × 150 mm Agilent Zorbax SB-C_{18} (5 μm) column. Semipreparative HPLC was run on an Agilent 1260 HPLC system using a 9.4 i.d. × 250 mm Agilent Zorbax SB-C_{18} (5 μm) column. A 4.7 i.d. × 250 mm Daicel Chiralpak AD-H (5 μm) column was employed for the chiral HPLC preparations of **1**–**3**. A silica gel column (200–300 mesh, Qingdao Marine Chemical Co. Ltd., China) and a reversed-phase C_{18} column (50 μm, Merck, Germany) were used for the preliminary separation of crude samples, and a Sephadex LH-20 column (Amersham Pharmacia Biotech AB, Sweden) was used for the final purification.

Plant Material. The dried bark (20 kg) of *S. indicus* was collected in Qinzhou (Guangxi Province, China) in September 2012 and was authenticated by Professor Fa-Nan Wei, Guangxi Institute of Botany. A reference voucher specimen (No. SIC20120925) was deposited at the Laboratory of Natural Products, Guangxi Normal University, China.

Extraction and Isolation. Air-dried, powdered bark (20 kg) of *S. indicus* was refluxed in 75% EtOH (3 × 2 h) to afford a crude extract (1.3 kg) that was subsequently suspended in H_2O (3 L) and successively extracted with petroleum ether (4 × 5 L), EtOAc (4 × 5 L), and *n*-BuOH (4 × 5 L). The bioactive screening of these extracts indicated that the EtOAc extract was the most cytotoxic against A549 and MCF-7 cells. The EtOAc extract (400 g) was divided into six fractions (A–F) by silica gel column chromatography (CC, 12 i.d. × 35 cm) eluting with a gradient of CH_2Cl_2/MeOH (100:0, 95:5, 90:10,

DOI: 10.1021/acs.jnatprod.6b00306
J. Nat. Prod. XXXX, XXX, XXX–XXX

80:20, 50:50, 0:100, v/v). Fraction B (60 g) was loaded onto a silica gel column (8 i.d. × 30 cm) and eluted with a gradient of CH_2Cl_2/MeOH (100:0−30:70, v/v) to afford 20 subfractions (B1−B20). Subfraction B1 (4 g) was separated on another silica gel column (4 i.d. × 15 cm) with a gradient of CH_2Cl_2/MeOH (100:0−10:90, v/v) to afford nine subfractions (B1-1−B1-9). Subfraction B1-1 (0.5 g) was fractionated by CC over Sephadex LH-20 with $CHCl_3$/MeOH (50:50, v/v) to yield **1** (45.0 mg) and **8** (8.5 mg). Racemic mixtures **1** and subfractions (B1-2, 40 mg) were further separated over a Chiralpak AD-H column with 80% *n*-hexane-isopropyl alcohol (0.8 mL/min) to afford a pair of enantiomers (−)-**1** (t_R = 9.4 min, 6.9 mg) and (+)-**1** (t_R = 15.6 min, 7.1 mg) and a pair of epimers **2** (t_R = 16.9 min, 6.3 mg) and **3** (t_R = 15.3 min, 6.1 mg), respectively. Subfraction B2 (20.0 g) was fractionated by CC over RP-C_{18} and eluted with mixtures of MeOH/H_2O with decreasing polarity (65:35−100:0, v/v) to afford seven fractions B2-(1−7). Separation of subfraction B2-1 (2.2 g) was done by semipreparative HPLC eluting with a gradient of MeOH/H_2O (20:80−25:75, v/v) and Sephadex LH-20 CC eluting with MeOH to yield **6** (7.9 mg), **7** (8.2 mg), and **9** (4.6 mg). Compounds **4** (6.2 mg), **5** (6.6 mg), **10** (5.3 mg), and **11** (7.8 mg) were obtained from subfraction B2-2 (1.5 g) via semipreparative HPLC eluting with a gradient of MeOH/H_2O (24:76−32:68, v/v).

*rac-Indidene A (**1**):* colorless crystals (MeOH); mp 156−157 °C; $[\alpha]_D^{25}$ +0.01 (*c* 0.4, MeOH); UV (MeOH) λ_{max} (log ε) 212 (4.30), 222 (4.11), 273 (3.92), 304 (3.83) nm; IR (KBr) ν_{max} 3403, 2968, 1715, 1601, 1472, 1382, 1163 cm^{-1}; for ^1H and ^{13}C NMR data, see Table 1; HRESIMS *m*/*z* 395.14560 (calcd for $C_{21}H_{24}O_6Na$, 395.14706).

*(+)-Indidene A (**1**):* yellow gum; $[\alpha]_D^{25}$ +31 (*c* 0.4, MeOH); ECD (MeOH) λ_{max} ($\Delta\varepsilon$) 289 (−7.8), 267 (0.43), 240 (2.7), 223 (−6.8), 207 (5.0).

*(−)-Indidene A (**1**):* yellow gum; $[\alpha]_D^{25}$ −31 (*c* 0.4, MeOH); ECD (MeOH) λ_{max} ($\Delta\varepsilon$) 289 (7.8), 267 (−0.43), 240 (−2.7), 223 (6.8), 207 (−5.0).

*Indidene B (**2**):* pale red powder; $[\alpha]_D^{25}$ +42 (*c* 0.4, MeOH); UV (MeOH) λ_{max} (log ε) 211 (3.9), 250 (3.81), 284 (3.60) nm; ECD (MeOH) λ_{max} ($\Delta\varepsilon$) 288 (11.4), 268 (14.1), 245 (−6.5), 218 (14.7); IR (KBr) ν_{max} 3410, 2939, 1741, 1730, 1690, 1503, 1398, 1147 cm^{-1}; for ^1H and ^{13}C NMR data, see Table 1; HRESIMS *m*/*z* 425.15618 (calcd for $C_{22}H_{26}O_7Na$, 425.15762).

*Indidene C (**3**):* yellow gum; $[\alpha]_D^{25}$ −32 (*c* 0.3, MeOH); UV (MeOH) λ_{max} (log ε) 210 (3.8), 250 (3.75), 284 (3.58) nm; ECD (MeOH) λ_{max} ($\Delta\varepsilon$) 286 (−8.1), 271 (2.8), 237 (−3.5), 227 (−1.8), 220 (−4.1), 210 (5.0); IR (KBr) ν_{max} 3409, 2938, 1740, 1730, 1691, 1504, 1398, 1146 cm^{-1}; for ^1H and ^{13}C NMR data, see Table 1; HRESIMS *m*/*z* 425.15618 (calcd for $C_{22}H_{26}O_7Na$, 425.15762).

*Indidene D (**4**):* white powder; $[\alpha]_D^{25}$ −84 (*c* 0.3, MeOH); UV (MeOH) λ_{max} (log ε) 254 (3.82), 290 (4.25), 330 (3.92) nm; IR (KBr) ν_{max} 3372, 2988, 1738, 1725, 1630, 1605, 1512, 1241, 1180 cm^{-1}; for ^1H and ^{13}C NMR data, see Tables 2 and 3; HRESIMS *m*/*z* 527.11545 (calcd for $C_{24}H_{24}O_{12}Na$, 527.11655).

*Indidene E (**5**):* white powder; $[\alpha]_D^{25}$ −95 (*c* 0.4, MeOH); UV (MeOH) λ_{max} (log ε) 262 (4.20), 286 (4.06), 342 (3.96) nm; IR (KBr) ν_{max} 3408, 2979, 1742, 1732, 1611, 1564, 1245, 1170 cm^{-1}; for ^1H and ^{13}C NMR data, see Tables 2 and 3; HRESIMS *m*/*z* 719.17989 (calcd for $C_{31}H_{36}O_{18}$ Na, 719.17993).

*Indidene F (**6**):* white powder; $[\alpha]_D^{25}$ −75 (*c* 0.4, MeOH); UV (MeOH) λ_{max} (log ε) 260 (4.12), 294 (3.97), 344 (3.86) nm; IR (KBr) ν_{max} 3421, 2945, 1736, 1730, 1615, 1460, 1245, 1072 cm^{-1}; for ^1H and ^{13}C NMR data, see Tables 2 and 3; HRESIMS *m*/*z* 689.16847 (calcd for $C_{30}H_{34}O_{17}Na$, 689.16937).

*Indidene G (**7**):* white powder; $[\alpha]_D^{25}$ −63 (*c* 0.4, MeOH); UV (MeOH) λ_{max} (log ε) 260 (3.73), 294 (3.80), 342 (4.03) nm; IR (KBr) ν_{max} 3429, 2968, 1742,1731, 1640, 1610, 1453, 1238,1069 cm^{-1}; for ^1H and ^{13}C NMR data, see Tables 2 and 3; HRESIMS *m*/*z* 747.21074 (calcd for $C_{33}H_{40}O_{18}Na$, 747.21123).

Acid Hydrolysis of 4−7. Compound **4** (2 mg) was dissolved in 1 M HCl (4 mL) and reacted at 80 °C for 4 h and extracted with EtOAc (3 × 5 mL). The aqueous layer was evaporated under a stream of N_2 to afford a neutral residue that was analyzed using TLC with EtOAc/pyridine/EtOH/H_2O (8:1:1:2) as the mobile phase. Glucose (R_f 0.37) was identified as the sugar component of **4** by comparison with authentic D-glucose (R_f = 0.36) and L-glucose (R_f = 0.39). Then, L-cysteine methyl ester hydrochloride (4 mg) and the neutral residue of the aqueous layer were dissolved in anhydrous pyridine (2 mL) and heated at 80 °C for 1 h. The reaction mixture was vacuum-dried and treated with *N*-trimethylsilylimidazole (0.4 mL) at 80 °C for 1 h. The reaction mixture was partitioned between water and *n*-hexane (each 3 mL). The *n*-hexane extract was analyzed by GC using a 0.32 mm i.d. × 25 m L-Chirasil-Val column. The detector temperature was kept at 280 °C, and the injector temperature was 250 °C. A temperature gradient was programmed to start at 160 °C and hold for 5 min, increase to 280 °C at 5 °C·min^{-1}, and hold for 10 min. The authentic samples were analyzed in the same way. Retention time for authentic silylated D-glucose and L-glucose were 19.09 and 19.25 min, respectively. The results of the GC analysis indicated that the sugar component of **4** was D-glucose (t_R = 19.08 min). The sugar components of **5**−**7** were established using the same procedure.

Computational Section. Conformational analysis was carried out using the VEGA ZZ3.0 program with Molecular Merck force field in Spartan 14 software.[24] A 1D potential energy surface scan of the C-6′−C-7′−C-1‴−C-6‴ dihedral angle in **2** and **3** was carried out at the semiempirical AM1 level. The conformers with relative energies within 2 kcal/mol (Table S1, Supporting Information) were optimized by density functional theory (DFT) at the B3LYP/6-31G (d) level. The B3LYP/6-31G(d) frequency calculations were performed to confirm the stability of each optimized conformer. The ECD spectra for the stable conformers were calculated by time-dependent (TD)-DFT at the B3LYP/6-311+G(2d,p) level using the polarizable continuum model in MeOH. The calculated ECD curves were generated using SpecDis 1.53 software (σ = 0.3 eV).[25] The final ECD spectra of (1′*R*,2′*S*)-**1**, (1′*S*,2′*S*)-**2**, and (1′*S*,2′*R*)-**3** were obtained based on the Boltzmann statistical contribution of each conformer and the experimental data. All DFT and TD-DFT calculations were conducted with Gaussian 09 program.[26]

X-ray Crystallographic Analysis of Indidene A (1). Crystals of indidene A (**1**) were obtained from its MeOH solution. Diffraction intensity data were collected on a Bruker APEX-II CCD diffractometer with Cu Kα radiation (λ = 1.541 84 Å). Structure solution was performed with program SHELXS-97 (direct method).[27] Structure refinement was done by full-matrix least-squares on F^2 (SHELXL-97),[27] with non-hydrogen atoms treated anisotropically. H atoms bonded to C and O were inserted in the ideal geometrical positions and refined as riding with *d*(C−H) = 0.93−0.98 Å, *d*(O−H) = 0.82 Å, and U_{iso}(H) = 1.2 *U*eq (C) or 1.5 *U*eq (O). Crystallographic data for indidene A (**1**) reported in the present study have been deposited at the Cambridge Crystallographic Data Centre (deposit number: CCDC 1471448). The data can be obtained free of charge at www.ccdc.cam.ac.uk or from the Cambridge Crystallographic Data Centre (12 Union Road, Cambridge CB2 1EZ, UK; Fax: (+44) 1223-336-033; or e-mail: desposit@ccdc.cam.ac.uk).

*Crystal Data of indidene A (**1**):* Moiety formula, 2($C_{21}H_{24}O_6$), CH_4O, M_r = 776.85, triclinic, space group $P\bar{1}$ (no. 2), *Z* = 2, *a* = 8.9728(4) Å, *b* = 13.5806(6) Å, *c* = 16.6376(7) Å, α = 93.952(2)°, β = 103.777(2)°, γ = 90.502(2)°, *V* = 1963.72(15) $Å^3$, *T* = 100 K, μ(Cu Kα) = 0.800 mm^{-1}, 35 146 reflections measured, 6401 unique (R_{int} = 0.0301), which were used in all calculations. The final R_1 was 0.0478, wR_2 was 0.1390, and *s* was 1.05 (all data).

Cytotoxicity Assay. The cytotoxic activities of the isolates were investigated using the MTT method.[28] The 1 × 10^4 cells suspended in 190 μL of media were added to each well of a 96-well microplate, incubated in 5% CO_2 atmosphere at 37 °C for 12 h, treated with a series of diluted compounds or paclitaxel for 48 h, and then cultured with 20 μL of 5 mg/mL MTT reagent for another 4 h. The formazan crystals in each well were then solubilized with 150 μL of DMSO. The absorbance was measured at 570 nm with a Bio-Rad 680 microplate reader. All experiments were repeated three times and each time in triplicate. The half-maximal inhibitory concentration (IC_{50}) values were acquired by fitting sigmoid curves with GraphPad Prism software (version 5.0).[29]

DOI: 10.1021/acs.jnatprod.6b00306
J. Nat. Prod. XXXX, XXX, XXX−XXX

■ ASSOCIATED CONTENT

Supporting Information

The Supporting Information is available free of charge on the ACS Publications website at DOI: 10.1021/acs.jnatprod.6b00306.

NMR and HRESIMS spectra of the new compounds and calculation data of **1**−**3** (PDF)

X-ray crystallographic data for compound **1** (CIF)

■ AUTHOR INFORMATION

Corresponding Authors

*(J. Li) Tel: +86-773-5803907. Fax: +86-773-2120958. E-mail: lijun9593@gxnu.edu.cn.

*(Y. Huang) Tel: +86-771-5883405. Fax: +86-771-5867737. E-mail: hy2002-2006@163.com.

Notes

The authors declare no competing financial interest.

■ ACKNOWLEDGMENTS

J.L. acknowledges the following grants for funding this project: The Program for Changjiang Scholars and Innovative Research Team in University (IRT1225); the Natural Science Foundation of Guangxi Province (2014GXNSFDA118008); the Open Research Fund program of Guangxi Key Laboratory of Traditional Chinese Medicine Quality Standards (GZZK201405); the Open Research Fund program of the Key Laboratory for the Chemistry and Molecular Engineering of Medicinal Resources (CMEMR2012−A21); and National Natural Science Foundation of China (21662004).

■ REFERENCES

(1) Zhang, S. S.; Wu, C. Y.; Cao, Z. Y. *Flora Reipublicae Popularis Sinciae*; Science Press: Beijing, 1998; Vol. *23*, pp 30−35.

(2) Zhao, A. H.; Yang, L. C.; Liu, G.; Wei, J. *Chin. Pharm. J.* **1999**, *34*, 368−369.

(3) Chen, J. M.; Qin, Y. N.; Cang, H. D. *Acta Acad. Med. Xuzhou* **1983**, *4*, 20−21.

(4) Wu, T. S.; Leu, Y. L.; Hsu, H. C.; Ou, L. F.; Chen, C. C.; Chen, C. F.; Ou, J. C.; Wu, Y. C. *Phytochemistry* **1995**, *39*, 383−385.

(5) Yang, X. W.; Xu, B.; Ran, F. X.; Wang, R. Q.; Wu, J. *Zhongxiyi Jiehe Xuebao* **2007**, *5*, 56−60.

(6) Panno, M. L.; Giordano, F.; Palma, M. G.; Bartella, V.; Rago, V.; Maggiolini, M.; Sisci, D.; Lanzino, M.; De Amicis, F.; Ando, S. *Curr. Cancer Drug Targets* **2009**, *9*, 469−481.

(7) Li, J.; Jin, B. F.; Zhang, Y. J.; Su, X. J.; He, X. C.; Huang, Y.; Huang, X. S.; Liao, R. Q.; Long, B. CN Patent ZL2006100 22463.3, 2011.

(8) Li, J.; Zhang, Y. J.; Jin, B. F.; Su, X. J.; Tao, Y. W.; She, Z. G.; Lin, Y. C. *Magn. Reson. Chem.* **2008**, *46*, 497−500.

(9) Lu, X. W.; Li, J.; Huang, C. P.; Meng, A. P.; Zhu, S. J. *J. Guangxi Normal Univ. (Nat. Sci. Ed.)* **2009**, *27*, 61−64.

(10) Zhu, S. J.; Li, J.; Meng, A. P.; Liu, Q. Y.; Huang, C. P.; Lu, X. W. *J. Guangxi Normal Univ. (Nat. Sci. Ed.)* **2010**, *28*, 33−36.

(11) Chen, Z. Z.; Li, J.; Wu, Q.; Yang, R. Y.; Li, L. Q.; Li, S.; Huang, J. G. *Guihaia* **2011**, *31*, 849−852.

(12) Huang, J. G.; Li, J.; Wu, Q.; Yang, R. Y.; Li, S.; Chen, Z. Z.; Li, L. Q. *Nat. Prod. Res. Dev.* **2012**, *24*, 780−783.

(13) Li, J.; Huang, Y.; Guan, X. L.; Li, J.; Deng, S. P.; Wu, Q.; Zhang, Y. J.; Su, X. J.; Yang, R. Y. *Phytochemistry* **2012**, *82*, 100−109.

(14) Chen, H.; Li, J.; Wu, Q.; Niu, X. T.; Tang, M. T.; Guan, X. L.; Li, J.; Yang, R. Y.; Deng, S. P.; Su, X. J. *Fitoterapia* **2012**, *83*, 643−649.

(15) Li, J.; Tang, M. T.; Wu, Q.; Chen, H.; Niu, X. T.; Guan, X. L.; Li, J.; Deng, S. P.; Su, X. J.; Yang, R. Y. *Nat. Prod. Commun.* **2012**, *7*, 599−602.

(16) Li, L. Q.; Li, J.; Huang, Y.; Wu, Q.; Deng, S. P.; Su, X. J.; Yang, R. Y.; Huang, J. G.; Chen, Z. Z.; Li, S. *Fitoterapia* **2012**, *83*, 303−309.

(17) Li, J.; Meng, A. P.; Zhu, S. J.; Tang, M. T.; Li, L. Q.; Li, S.; Chen, Z. Z.; Huang, J. G. CN Patent HZ201110094274.8, 2012.

(18) Li, J.; Meng, A. P.; Guan, X. L.; Li, J.; Wu, Q.; Deng, S. P.; Su, X. J.; Yang, R. Y. *Bioorg. Med. Chem. Lett.* **2013**, *23*, 2238−2244.

(19) Rastogi, S.; Kulshreshtha, D. K.; Rawat, A. K. S. *Evid.-Based Compl. Alt. Med.* **2006**, *3*, 217−222.

(20) Fan, L.; Wang, Y.; Liang, N.; Huang, X. J.; Li, M. M.; Fan, C. L.; Wu, Z. L.; Li, Y. L.; Ye, W. C. *Planta Med.* **2013**, *79*, 1558−1564.

(21) Iqbal, P. F.; Bhat, A. R.; Azam, A. *Eur. J. Med. Chem.* **2009**, *44*, 2252−2259.

(22) Tsukamoto, H.; Hisada, S.; Nishibe, S. *Chem. Pharm. Bull.* **1985**, *33*, 396−399.

(23) Laplante, S. R.; Edwards, P. J.; Fader, L. D.; Jakalian, A.; Hucke, O. *ChemMedChem* **2011**, *6*, 505−513.

(24) *Spartan 14*; Wavefunction, Inc.: Irvine, CA.

(25) Bruhn, T.; Hemberger, Y.; Schaumlöffel, A.; Bringmann, G. *SpecDis*, version 1.53; University of Wuerzburg, 2011.

(26) *Gaussian 09*, revision C.1; Gaussian, Inc.: Wallingford, CT, 2010. A full list of authors can be found in the Supporting Information.

(27) Sheldrick, G. M. *Acta Crystallogr., Sect. A: Found. Crystallogr.* **2008**, *A64*, 112−122.

(28) Mosmann, T. J. *J. Immunol. Methods* **1983**, *65*, 55−63.

(29) *GraphPad Software*, San Diego, CA.

DOI: 10.1021/acs.jnatprod.6b00306
J. Nat. Prod. XXXX, XXX, XXX−XXX